2016

A Computational Model of Cell Movement on Surface with Concave Corner Architecture and Viscoelastic Effects

Kaiyuan Peng
Lehigh University

A Computational Model of Cell Movement on Surface with Concave Corner Architecture and Viscoelastic Effects

By

Kaiyuan Peng

A Thesis

Presented to the Graduate and Research Committee

of Lehigh University

in Candidacy for the Degree of

Master of Science

in

Mechanical Engineering and Mechanics

Lehigh University

May, 2016

This thesis is accepted and approved in partial fulfillment of the requirements for the Master of Science.

_____
Date

_____
Professor Arkady Voloshin, Thesis Advisor

_____
Professor Gary Harlow, Chairperson of Department

ACKNOWLEDGEMENTS

I would like to thank my advisor, Professor Arkady Voloshin, for his patient guidance. Professor Voloshin inspire me new ideas and guide me to investigate problems critically in the past one year I working with him. I would also like to thank Mr. Dafu Gao, Mrs. Jie Sheng and Mr. Emre Akoz for their generous help.

Finally, my special thanks to my parents for their continuous encouragement to me.

Table of Contents

List of Tables

List of Figures

Abstract

Living cells respond to the outside physical environment by changing their geometry and location. It is crucial to understand the mechanism of cellular activities, such as cellular movement and utilize cellular properties, such as cellular viscoelasticity by both experimental and computational means.

A computational model is developed as a tensegrity structure, which not only consists of the cytoskeleton, but also models the cellular nucleus and lamellipodia. This model is based on the use of the isolated components consisting of a set of continuous compression components and a set of continuous tension components. To investigate the influence of surface topography on cellular movement, some representative cases were designed and simulated. By defining strain energy as a main criterion to estimate the stability of a cell at various locations, the results show that cells have a tendency to move towards and stay on the side wall, and they also have a tendency to leave the concave corner. The simulation results are in agreement with the experimental evidence.

In addition, a computational approach to simulate cellular viscoelasticity was also developed. By defining the parameters of the Prony series and based on the 30-members tensegrity structure, this cellular model shows a very similar viscoelastic behavior compared with the experimental data. Thus, the proposed model and approach is a valuable tool for understanding the mechanics of cells.

Introduction

Living cells have the capability to respond to their external physical environment by changing their geometry and location.[1] These changes are influenced by the cells' internal balance as they need to maintain structure stability and molecular self-assembly. Due to mechanical loads or cell-generated forces that appear during the cells' migration, geometry and energy changes in the cells takes place.[2] These are mechanical signals that cells sense are transduced via the cytoskeleton structure. This interconnected structure, namely the cytoskeleton, also serves as a stabilization of cell shape due to its network structure which consists of tubules and filaments.

In the studies conducted by Ingber DE[3], [4] tensegrity structures are used to predict cells' response to mechanical signals transmitted by a cytoskeletal structure. Mechanical signals may transduce into biological or chemical responses by varying the force-dependent scaffold geometry or molecular mechanics.[4] In addition, the mechanism of mechanical energy transduction is also provided by tensegrity.[3]

To investigate the biological signal transduction and the cells' response to different physical environments, much experimental research was published recently.[5], [6], [7], [8], [9] By culturing normal rat kidney epithelial and 3T3 fibroblastic cells on a collagen-coated polyacrylamide substrate, the cells' response to the stiffness of the surface was investigated. The result showed that cells on flexible substrates (relatively soft substrates) showed reduced spreading

compared with cells on rigid substrates. The focal adhesions on flexible substrates were highly dynamic whereas those on rigid substrates were more stable.[5]

Other research focusing on eukaryotic cells concludes that the ultimate shape of cells is defined by cycles of mechanosensing, mechanotransduction, and mechanoresponse. Local sensing of cellular geometry or force is transduced into biochemical signals that result in cell responses even for cell-level formation and cells' migration. These responses regulate cell growth, differentiation, shape changes, and cell death.[6]

Research on cell signal transduction mechanisms in guard cells was conducted by Schroeder, Allen in 2011.[7] Guard cells are the cells surrounding each stoma which help to regulate the rate of transpiration. Their signal transduction mechanisms integrate light signals, water status temperature, and other environmental conditions to regulate plant survival under diverse conditions. This study showed the manipulation of guard cell signals would not only affect the cells' movements but also control more complex functions of the cell.[7]

The focal adhesion is also an important effect factor on cells' migration, movement, and signaling, which serves as a force and signal transduction media between the actin cytoskeleton and the extracellular matrix.[8], [9]

In the study of the influence of surface topography on cell responses to micropatterned substrates, a human epithelial cell was used.[10] This experiment indicated that heterogeneity of cells' distribution at different locations was caused by their movement behavior at the concave and convex corners of pit and pillar

substrates. It was concluded that the anisotropic topographical features of concave and convex architecture affects cells' spatial growth and distribution.[10]

In the study of cellular behavior on concave and convex microstructures fabricated from elastic PDMS membranes,[11] cells' distribution is related to deformation of the plasma membrane and the formation of stress fibers. The experimental results showed that the cell on the micropatterned substrate actively "escaped" from concave patterns, but not from the convex.[11]

Except for the experimental works, a number of computational cell models were developed in recent years in order to provide an explanation of the mechanism of cells' responses to an external environment.[12], [13], [14], [15], [16], [17], [18] The computational models can mainly be divided into the continuum and the microstructure models.

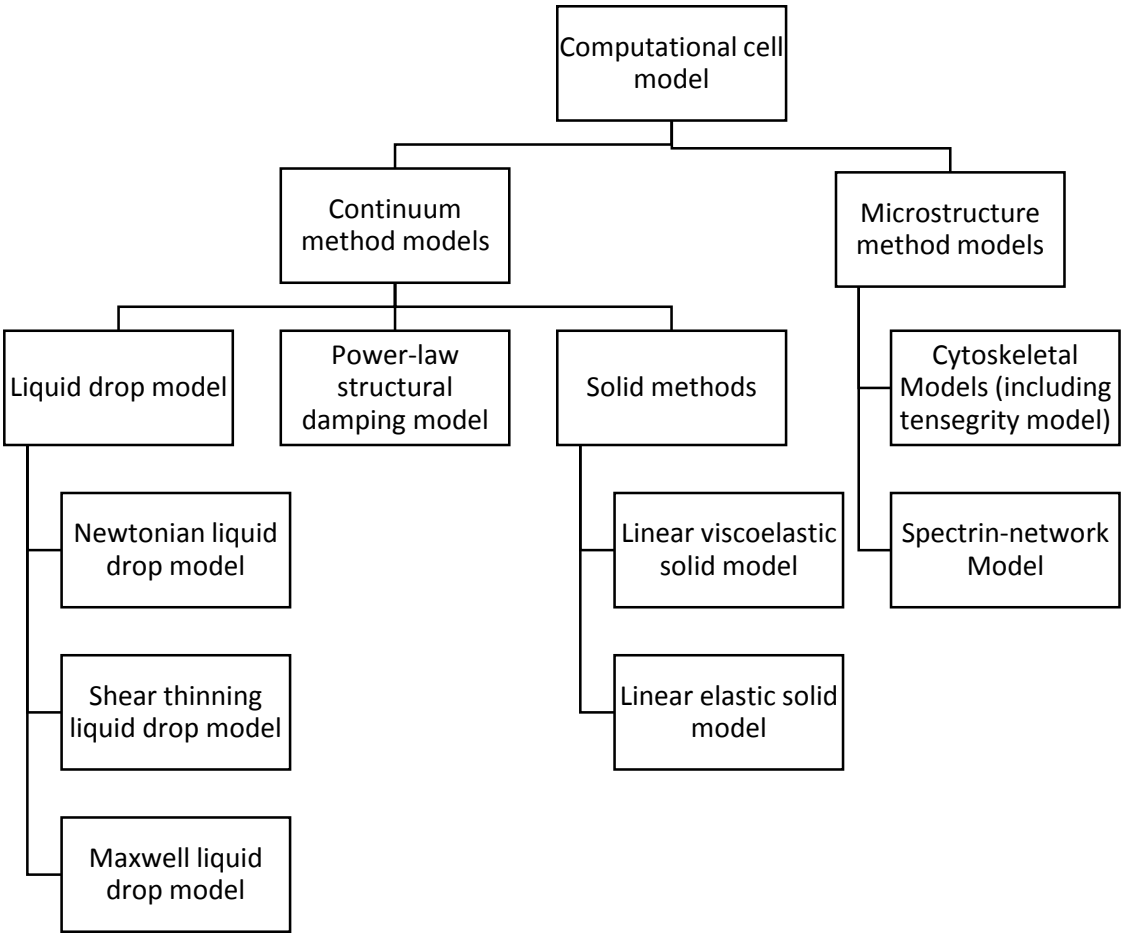

Figure 1 The categories of the computational cell models

The continuum models are represented by the liquid drop model, the power-law structural damping model, and solid models. The liquid drop model is one of the most popular models for analysis of cellular deformation,[19] which is widely applied to the cell. Based on the Newtonian viscous liquid properties, the Newtonian liquid drop model was developed by Yeung and Evans (1989) in order to simulate the flow of such liquid-like cells into the micropipette.[20], [21] Another widely used type of liquid drop model is the Maxwell model. Newtonian or

Newtonian-like models can account for large deformation in order to explain the initial rapid elastic-like entry during the micropipette aspiration of the cell. Dong *et. al.* (1988) applied the Maxwell liquid drop model to study the small deformation.[22] This model for a passive leukocyte consisted of a pre-stressed cortical shell containing a Maxwell fluid.

On the other hand, in order to simulate the elastic and viscoelastic behavior of cells, two types of solid models were developed: the linear viscoelastic solid model and the linear elastic solid model.[23] These solid method models were developed in order to be devoted to the small-strain deformation characteristics of leukocytes.

The last, but the most important category related to our topic, is the microstructure method model. Both the cytoskeletal model and spectrin-network model are categorized as micro-structure models. Based on the behavior of the micro filamentous structure, the cytoskeletal models were developed and are based on the tensegrity model, tensed cable network model, and open-cell foam model.[24] The cytoskeleton serves as the main structural component in this approach while the whole pre-stressed cable network is devoted to modeling the deformability of cells.[24], [25], [26] The tensegrity architecture was first described by Buckminster Fuller in 1961.[27] The discontinuous-compression, continuous-tension structural systems were developed and were named the Geodesic Tensegrity.[28], [29]

In this study, we employ a new type of tensegrity model containing cells' nucleus and lamellipodia in order to simulate their movement on a micropatterned

substrate with concave architecture and use the total strain energy as a main criterion to evaluate the cells' movement tendency at various locations. Also, after defining the viscoelastic properties of microfilament components, simulation is implemented in order to analyze the viscoelastic behavior of a cell.

1. Model description

1.1 Classical tensegrity model for living cell

1.1.1 Tensegrity Structure

Tensegrity is a structure based on the use of the isolated components consisting of a set of compression members and a set of continuous tensile members in such a way that the compressed members (usually bars or struts) cannot touch each other and the pre-stressed tensile members (usually cables) delineate the system spatially and make the total structure self-sustainable. It is clearly seen in Figure 2 that the tensegrity structure is composed of isolated stainless steel bars and suspended in space by high tension cables.[30]

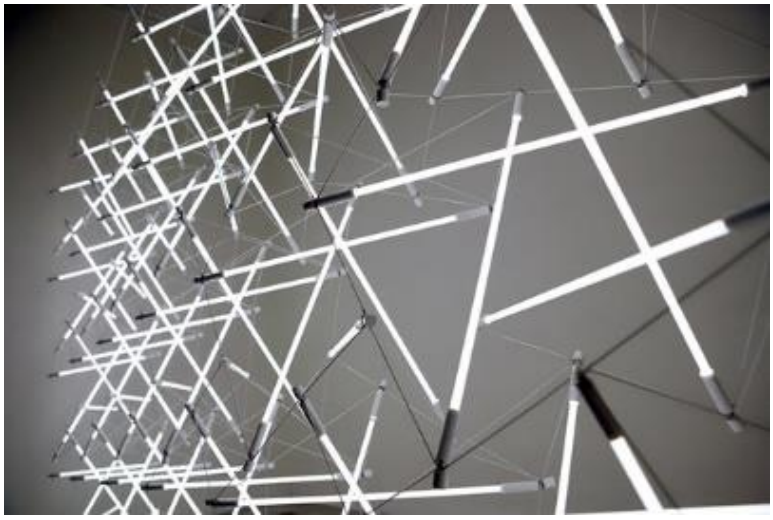

Figure 2 A tensegrity structure[31]

1.1.2 Classical tensegrity cell model

Several research papers illustrate that a specific tensegrity structure can model the mechanical behavior and geometry deformation of living cells. One specific tensegrity cell model consists of 30 components, including 6 struts, which represent the micro-tubulous members in the cytoskeleton, and 24 cables, which

represent the micro-filamentous members or intermediated filamentous members in the cytoskeleton (CSK). All struts carry compression loads while all filaments carry tension loads to form a stable structure in space.[32], [33], [34]

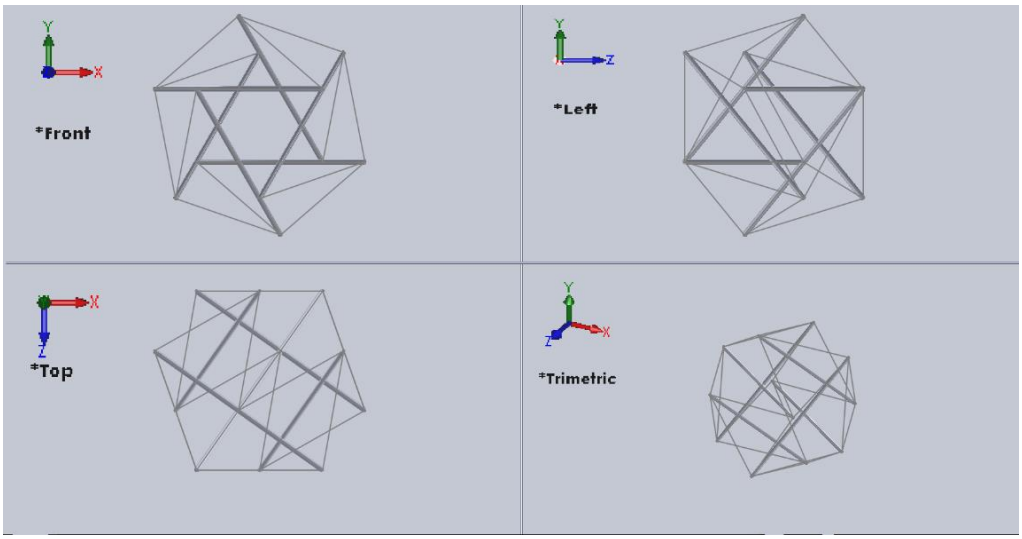

Figure 3 Classical cell tensegrity structure

In this model, node 1, node 2 and node 3 are attached to the surface. Typically, one node needs to be fixed to the surface to simulate the focal adhesion. The rest of the nodes are free and will exhibit morphing or a geometry change when external or internal forces are applied to the cells.[35]

1.2 Cell model with nucleus and lamellipodia

1.2.1 Geometry of new cell model

In this structure, a new type of cell model is introduced to simulate the cells' surface movement. Not only the cytoskeleton but also the nucleus and the lamellipodia are involved.

It is necessary to model the lamellipodium since it has a very important role in the cells' movement. Biologically the lamellipodium is a cytoskeletal protein actin protruding from the leading edge of the cell. When the cell moves, the leading edge of this structure extends first and then propels the whole cell-level body.

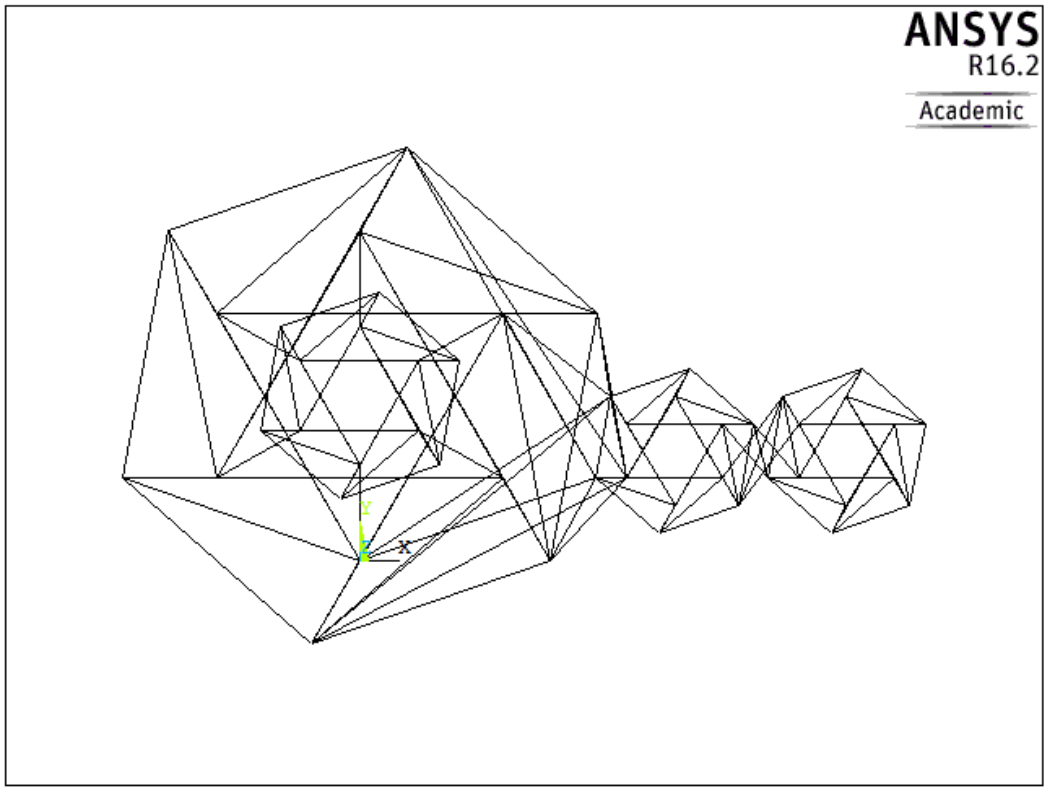

Figure 4 Cell model with nucleus and lamellipodium (x-y plane)

We are using ANSYS APDL Academic 16.2 as the computational model of this structure. "Link 180" was selected to model the micro-filamentous members and "Beam 188" to model the micro-tubulos members. In Figure 4, the left-hand side refers to the cytoskeleton and nucleus, while on the right-hand side, the long strip structure represents the lamellipodium.

Similar to the classical tensegrity cell structure, the cytoskeletal structure also contains 30 members that consist of 6 struts and 24 cables. The nucleus is generated by the similar structure but the dimension are smaller than the cytoskeleton. The lamellipodium is formed by two tensegrity structures of the same size that are oriented in a row.

After defining the geometry of the main structures, connections between each structure need to be created. To connect the cytoskeleton and nucleus 6 tensile members are selected, 12 cables are used to connect the cytoskeleton and lamellipodium, and another 6 cables are used to connect the right-hand part and left-hand of the lamellipodium.

1.2.2 Mechanical properties of cellular members

The mechanical properties of microtubules and microfilaments were assigned on the basis of the experiment implemented by Mickey *et. al.*[36]In our study, most of the parameters of cells' properties were followed by this experiment, but the value of the cross section was enlarged to make the whole structure more stable under the external driving force. The physical and mechanical properties of the cellular members are displayed in Table 1.

Table 1 Physical and mechanical properties of the cellular members in the cell model

Properties	Micro-tubules	Micro-filaments
Element type (Defined in ANSYS APDL)	Link 180	Beam 188
Radius (nm)	36.0	15.00
Cross section area (nm^2)	4070	707
E (GPa) (Elastic modulus)	1.200	2.60
Poison's ratio	0.30	0.30

1.2.3 Initial and boundary conditions

After defining the geometry and mechanical properties of cellular members, appropriate initial and boundary conditions need to be set. For a tensegrity structure, one import factor that allows to maintain the shape is a pre-stress. Pre-stress is generated by the tensile forces in microfilaments. These tensile forces will keep each microfilament under tension and exert a compressional force on compressional elements via each node. In addition, the complementary force balance between the tension and compression elements is important. In this study, there are 48 nodes that are distributed in a three-dimensional space.

Initial conditions (Figure 5) are defined to simulate the cells' focal adhesion. In cell biology, focal adhesions are large macromolecular assemblies through which mechanical force is transmitted between the extracellular matrix (ECM) and an interacting cell. In this study, node 3 is fixed to the surface, i.e., node 3 is constrained in all translational and rotational degrees of freedom. Node 1 and node 2 are constrained in a z-direction and all rotational degrees of freedom, which allows them to move in an x-y plane. For the rest of the bottom nodes, nodes 25, 26, 27 and nodes 46, 47, 48, the type of constraint set is the same as node 1 and node 2, which means these nodes can slide in on an x-y plane but cannot leave the surface plane or cross below the bottom surface.

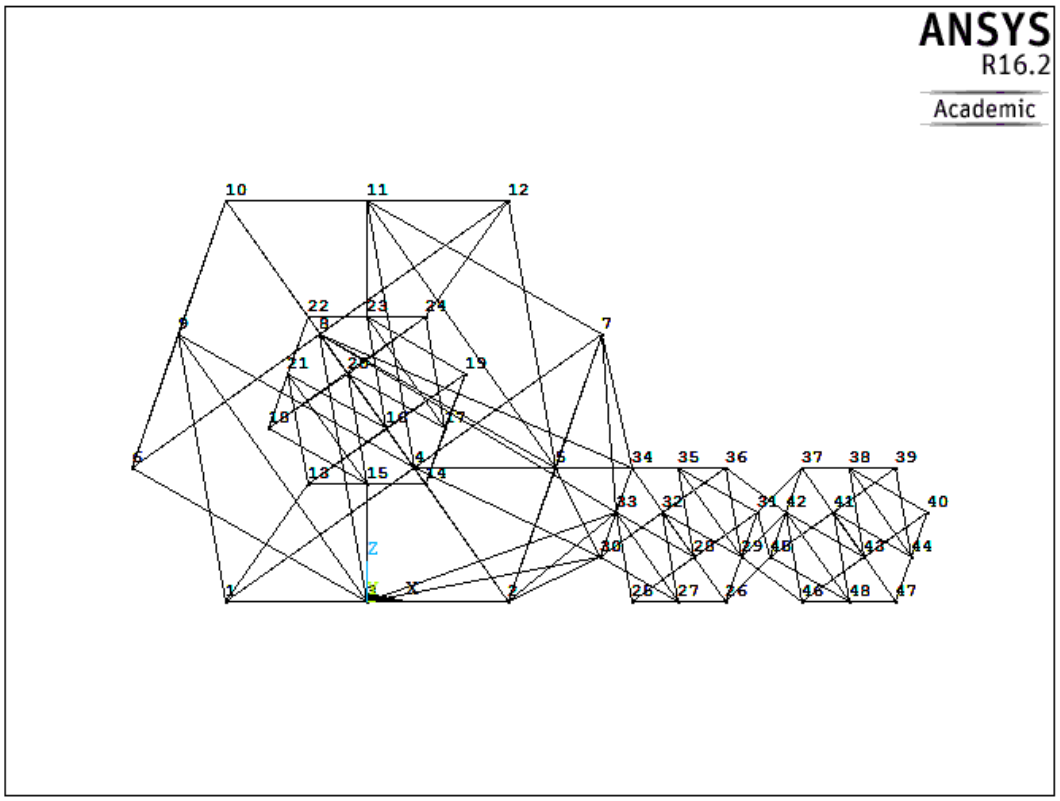

Figure 5 Cell structure in x-z plane to show the initial and boundary conditions

1.2.4 Energy calculation method

To evaluate the cells' stability when a single cell is moving across the surface, the total energy of the cell approach is evaluated. A higher internal elastic energy means the cell is not likely to stay in this location and will try to move to another location that will result in a lower energy. If the cell is at the lowest energy level compared to all other cases, this is called a stable state for the cell.

After applying pre-stress or external force, a displacement will occur. The following are the governing equations for the displacement and corresponding strain energy change.

Mathematically, the displacement is expressed by the equation,

$$[K]\{d\} = \{L\} \quad (1)$$

where [K] is the stiffness coefficient matrix for each element, {d} is the vector for each nodal displacement and {L} is the vector of force acted on each node.

To calculate the stiffness of the tensile element or compression element, the mathematical expression of elastic modulus needs to be included.

$$E = \frac{\sigma}{\varepsilon} = \frac{F / A}{\Delta L / L_0} \quad (2)$$

where E is the elastic modulus, also called Young's modulus, σ is the tensile stress and ε is extensional strain.

Simplifying equation 2,

$$E = \frac{FL_0}{A\Delta L} \quad (3)$$

which denotes the cross section area as A, initial length as L_0, axial force as F and change in length as ΔL.

Based on the definition of stiffness, which is the ability to resist deformation due to external force, the stiffness is defined as a ratio of external force to deformation.

$$K_i = \frac{F_i}{\Delta L_i} \quad (4)$$

K*i* is the coefficient of stiffness.

Combining the equations above,

$$K_i = \frac{E_i A_i}{L_i} \tag{5}$$

To calculate the total elastic energy of the cell modeled by the tensegrity structure, the energy in each element, which refers to the strain energy of microtubules and microfilaments, needs to be added up. The formation of the governing equation to calculate the total energy is,

$$E = E_s + E_c \tag{6}$$

$$E_s = \frac{1}{2}\int_V \{\sigma\}_s \{\varepsilon\}_s dV \tag{7}$$

$$E_c = \frac{1}{2}\int_V \{\sigma\}_c \{\varepsilon\}_c dV \tag{8}$$

where E denotes the total energy of the cell, E_s denotes the total energy in all tensile elements and E_c denotes the total energy stored in all compression elements. Meanwhile, $\{\sigma\}_s$ refers to the components of stress in each tensile filament, $\{\varepsilon\}_s$ refers to the components of strain of each tensile filament, $\{\sigma\}_c$ and $\{\varepsilon\}_c$ refers to the components of stress in each compression tubule and the components of strain of each compression tubule respectively.

2. Effect of pre-stress on cell model

2.1 Simulation process

To evaluate the pre-stress influence on the cell behavior, a tensegrity cell model with a cytoskeleton and a nucleus was used (Figure 6). The outer form of

the structure is the cytoskeleton and the inner tensegrity structure in the central part of the cytoskeleton is the nucleus.

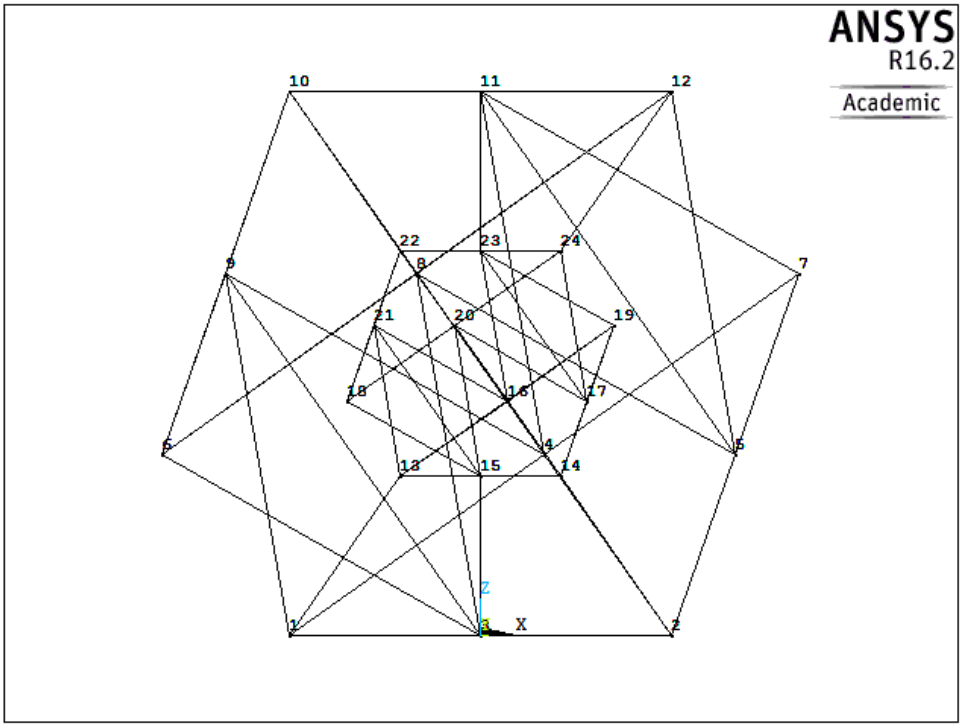

Figure 6 Cell model consisted of cytoskeleton and nucleus

First pre-stress is applied. A higher pre-stress and a lower pre-stress are applied to each node respectively (Table 2). After setting all other external conditions to be the same, a downward in the negative z direction force of $0.5*10^{-11}$ N is applied to node 12 in both cases.

2.2 Result

As shown in Table 2, after applying the same downward force to node 12 in each case respectively, the resultant displacement for node 12 varies.

Table 2 The location of node 12

Pre-stress (N)	**Original z-coordinate without pre-stress for node 12 (μm)**	**z-coordinate with only pre-stress for node 12 (μm)**	**Deformed z-coordinate for node 12 (μm)**
TENS = 0.80e-13 COMP = -1.92e-13	14.72	14.71	14.28
TENS = 0.80e-12 COMP = -1.92e-12	14.72	14.65	14.60

In the case of a higher pre-stress, the value of tension force is $0.\ 8*10^{-13}$ N, and the compression force is equal to $-1.92*10^{-13}$ N (a negative sign denotes compression). The original coordinate shows the geometry without pre-stress. After applying pre-stress, the total structure will deform, resulting in a slight change to node 12 position in the z direction. In the next step, a downward force, $F = -0.5*10^{-11}$ N, is applied, where the negative sign denotes the direction of the force as vertically downward. The deformed location of node 12 is 14.28 μm in the z-direction.

In the case of a lower pre-stress, the value of the tension force is $0.\ 8*10^{-12}$ N, and the compression force is equal to $-1.92*10^{-12}$ N, which is 10 times larger than the first case. This shows a larger displacement for node 12 after applying pre-stress than in the first case. The reason is a larger value of pre-stress makes this tensegrity cell model stiffer. Next, as in the first case, $F = -0.5*10^{-11}$ N is applied downwards to node 12. The final z- coordinate given is 14.60 μm.

By comparing the first case to the second, although a larger value of pre-stress gives a larger shrinkage initially, it also makes the model stiffer, while a

smaller pre-stress makes the cell model softer. This result is supported by the data in Table 2. When applying the same force, a stiffer structure deforms less while a softer structure deforms more.

The displacement plots show the relationship between the pre-stress and the load (Figures 7 and 8). The solid black line represents the original geometry without any external force applied and the solid blue line shows the deformed shape of this cell after applying pre-stress and external force.

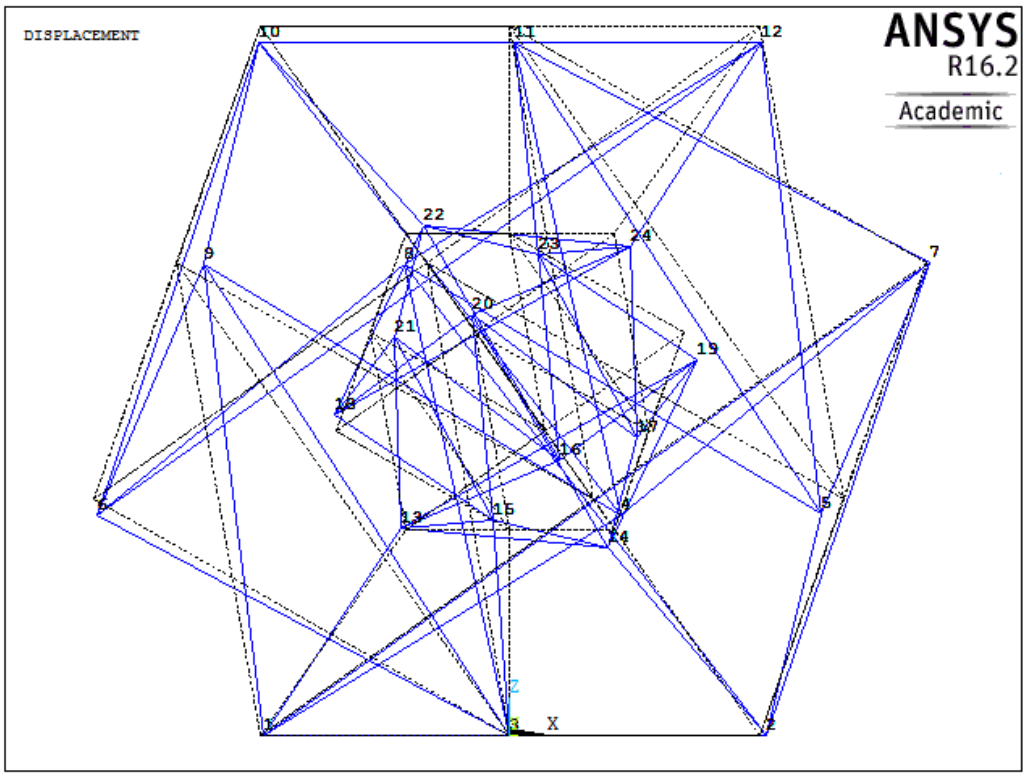

Figure 7 Deformed and unreformed plot with a lower pre-stress

After applying the vertical force to the node 12, all nodes on the top surface move downward. For the case of a higher pre-stress, (Figure 8) only a slight change in shape can be seen since the structure is much stiffer. After

zooming in, the downward displacement of node 12 can be observed in the deformed plot, while the displacements of node 10 and node 11 which are in the same level plane are negligible.

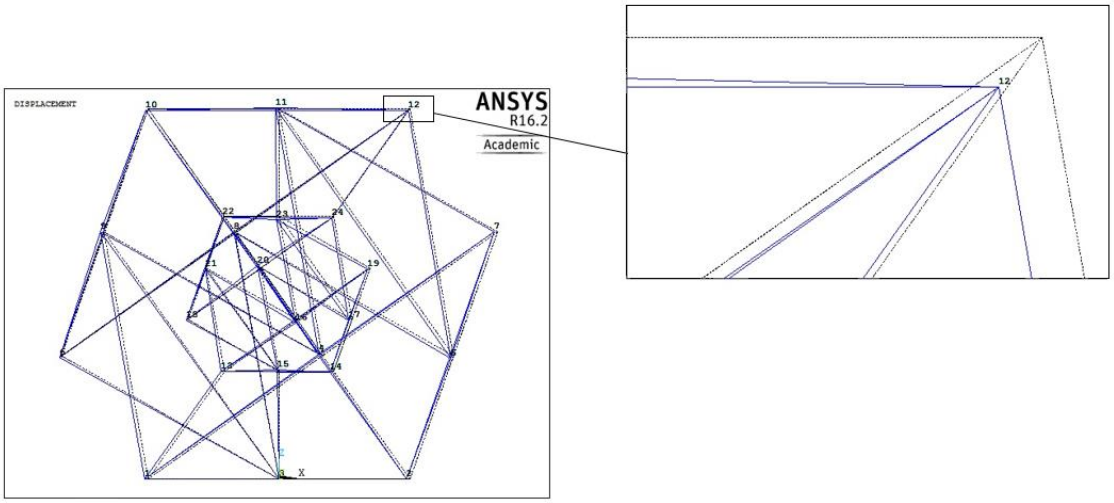

Figure 8 Deformed and unreformed plot with a higher pre-stress

3. Simulation of the cell movement

3.1 Simulation process

To investigate the tendency of cell movement on the surface, especially for the surface with concave architecture, a tensegrity cell model with a nucleus and a lamellipodium structure, as shown in section two, was used. The goal of this study is to find the relationship between the cell's location and the total energy change during their movement along the substrate.

In this section, simulations are performed on the flat surface and the surface with a concave corner. Several cases are designed and simulated, such as, the cell moves forward on the flat surface, the cell encounters the wall when it reaches the concave corner, the cell directly moves up when cell becomes close to the vertical wall and it moves sideways when it approaches the wall.

In all cases, the effect of gravity is neglected. Node 3 is always anchored to simulate focal adhesion. The strain energy of the cell changes when the lamellipodium extends and the cell body moves. Based on the criterion of minimum energy, the possibility and tendency of the cell's location will be shown.

3.1.1 Cell moves forward along the flat surface

The first step is to impose the initial constraints. Node 3 is fixed in all directions and all other bottom nodes are fixed in the z-direction to make sure all bottom nodes can only move along the surface. Then, the pre-stress is applied. The pre-stress will result in a slight change of total shape and in the length of each strut and filament. Based on the biological study of the cell's movement, the lamellipodium always extends first and then it pulls the main cell body forward.

So in this study, after applying pre-stress, two forward nodes (node 40 and node 44 shown in Figure 9) on the forward edge of the lamellipodia are selected. We applied one micron and two micron displacement along the x-direction to these nodes, parallel to the flat surface. Figure 9 (front view) and Figure 10 (top view) show the cell geometry after it moves forward one micron, where the solid blue line is the cell's deformed shape after one micron movement and the solid black line is the original shape. Figure 11 shows the deformation of the cell when it moves forward 2 microns.

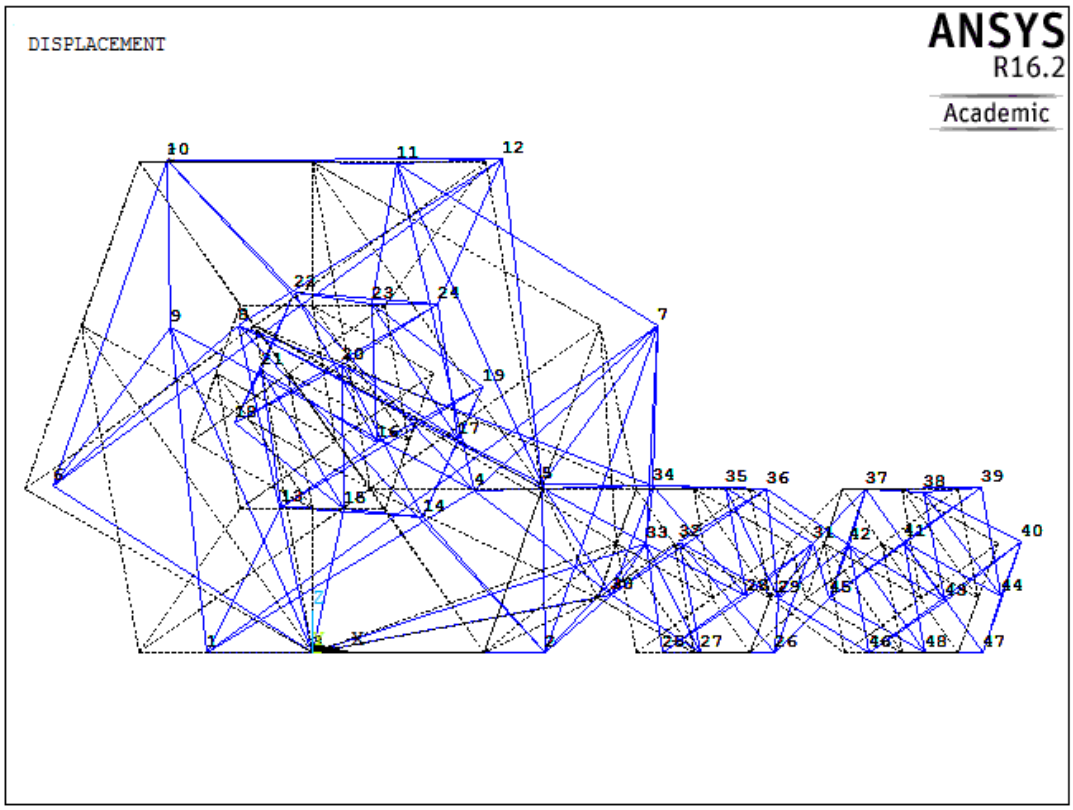

Figure 9 Cell model moves forward for one micron (x-z plane)

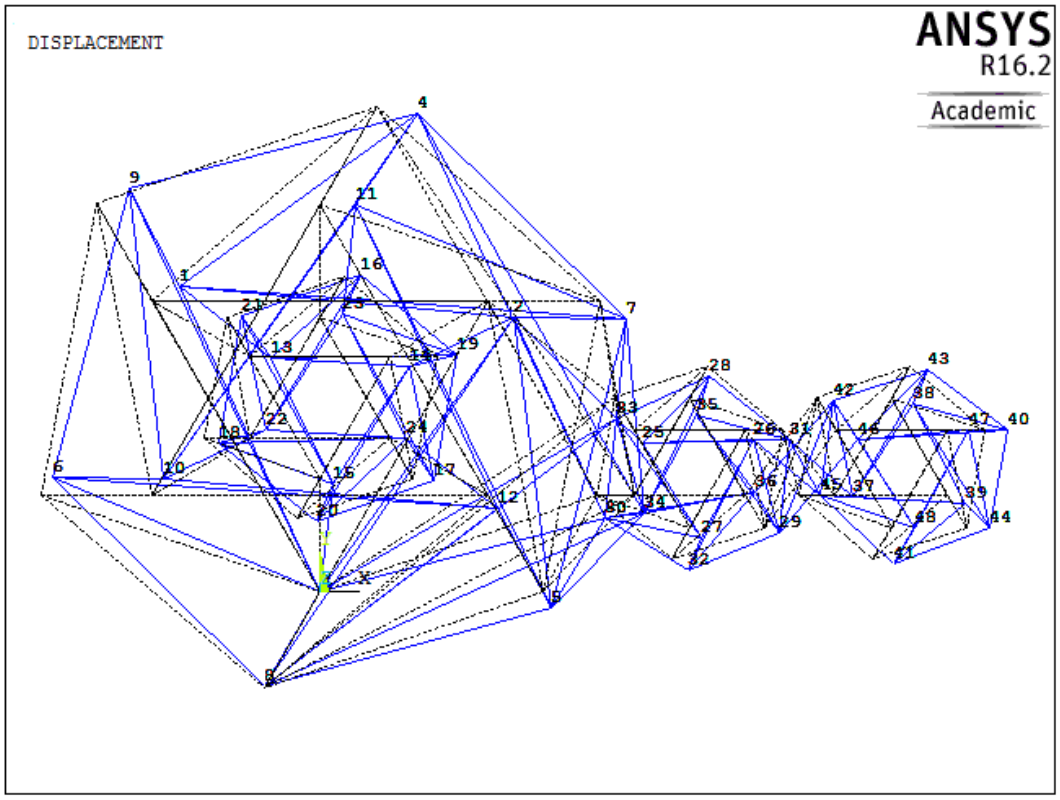

Figure 10 Cell model moves forward for one micron (x-y plane)

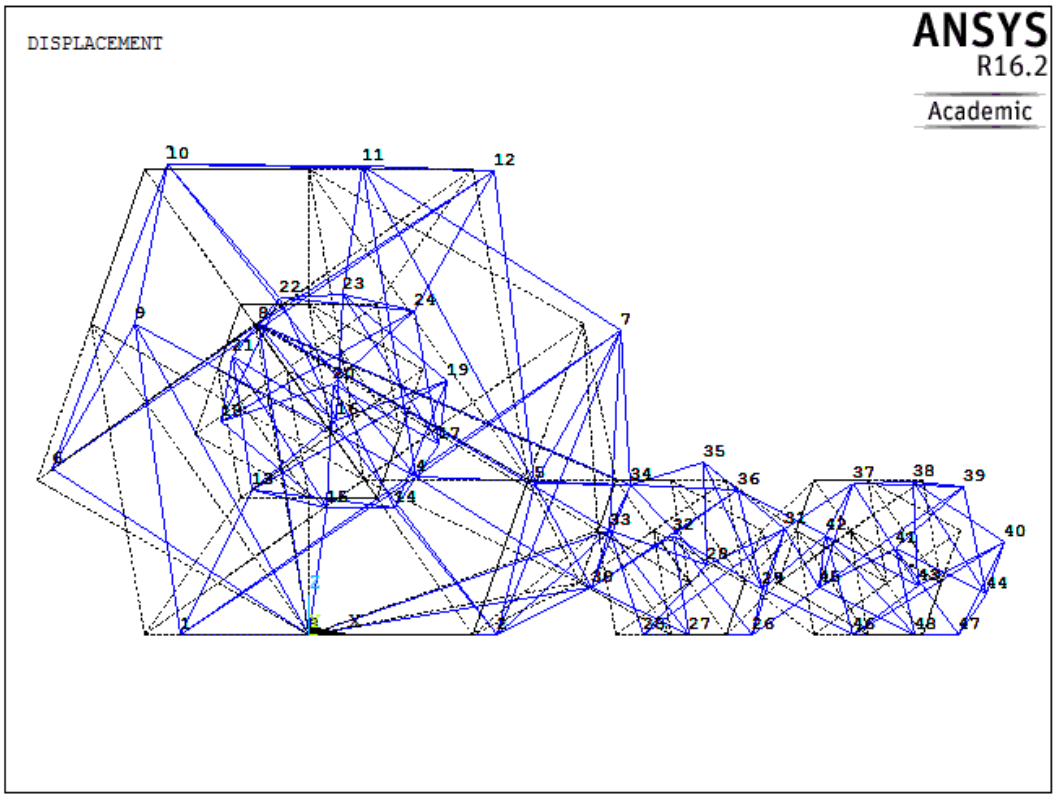

Figure 11 Cell moves forward for two micron (x-z plane)

3.1.2 Cell encounters the wall

Let us assume that the cell is currently in the bottom of the flat pit as shown in Figure 12.

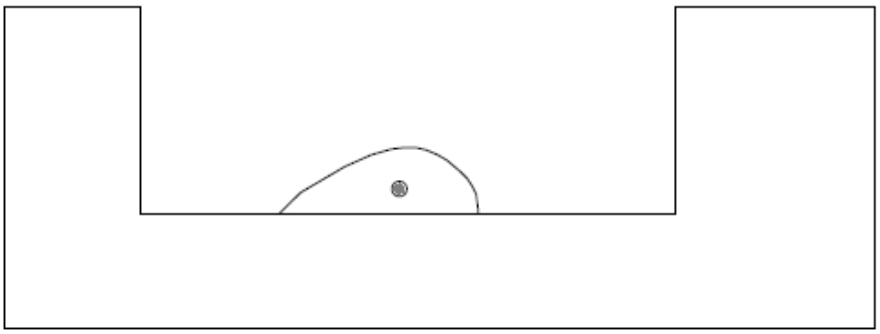

Figure 12 Cell in a pit

It is not unusual to expect that the cell would encounter the vertical wall after some movements. Then there must be an energy change after cell encounters the wall.

The following procedure was developed to simulate the encountering process. It is assumed that the cell is at the bottom surface originally and the side wall is at the distance of one micron from the cell's original location. Assuming that the cell does not know there is a wall in its path, what will happen if it initially wants to move directly for two microns? If the cell wants to move, it needs to generate inside forces which will drive it to move. If the cell wants to move directly for two microns it must generate a force which will guarantee the two micron movement. The same situation occurs if the cell only wants to move for one micron. The inside forces will be generated to drive the cells for one micron movement. Thus, if the cell wants to move for two microns initially, but encounters a wall only after one micron movement, some remaining forces must be inside the cell that will push against the wall.

When applying a two micron displacement to the forward nodes, node 40 and node 44, the lamellipodium structure will extend for two microns and pull the main cell body forward. After the cell's movement, we can obtain a list of nodal force values from node 1 to node 48, which are the corresponding to the inside forces for the deformed cell. The nodal forces in the x, y and z coordinate can be evaluated, let's call them F_2. Back to the initial configuration, then give two forward nodes one micron movement and calculate the corresponding nodal forces on each node after this one micron movement, they are called F_1. The remaining potential forces are calculated by,

$$\{F_3\} = \{F_2\} - \{F_1\} \qquad (9)$$

where $\{F_3\}$ is a 48 by 1 vector which denotes the remaining force.

To simulate the situation when the cell moves forward but encounters the wall in its pathway, in the beginning a one micron movement in the x-direction is given. Then we apply the remaining forces $\{F_3\}$ to each node to simulate the effect of encountering the wall. The total strain energy of the cell after it encounters the wall is calculated and stored.

3.1.3 Cell moves up or sideways

When the cell encounters the wall the next possible movement could be up the wall or sideways. In the case of upward movement, one micron forward movement is given to the forward nodes, node 40 and node 44, and the constraints in the y direction are also made to keep the forward nodes only moving in the x direction. After the front side of the lamellipodium contacts the wall, one micron movement in a positive y direction or positive z direction is applied to the front two nodes respectively. To simulate the case of the cell's upward movement, the constraints of three bottom nodes in the z direction are released to ensure the lamellipodium can move off the surface. As a result, Figure 13 (front view) shows the cell's upward movement and Figure 14 (top view) shows the cell's sideways movement.

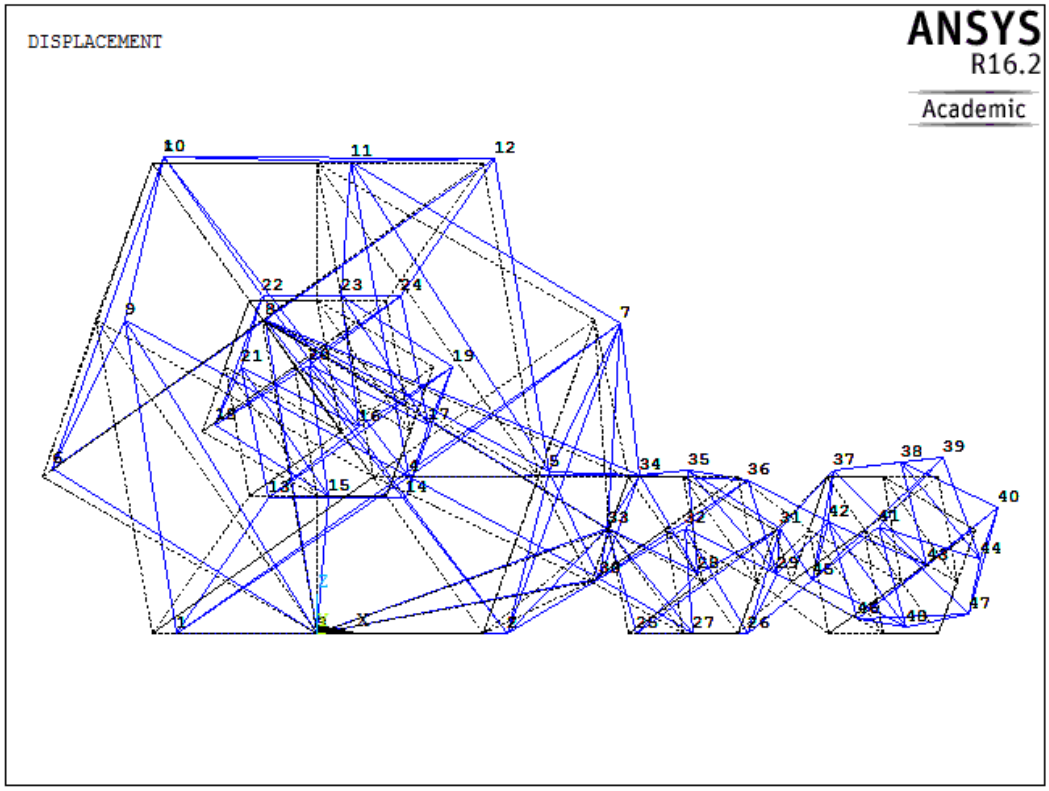

Figure 13 Cell moves up (x-z plane)

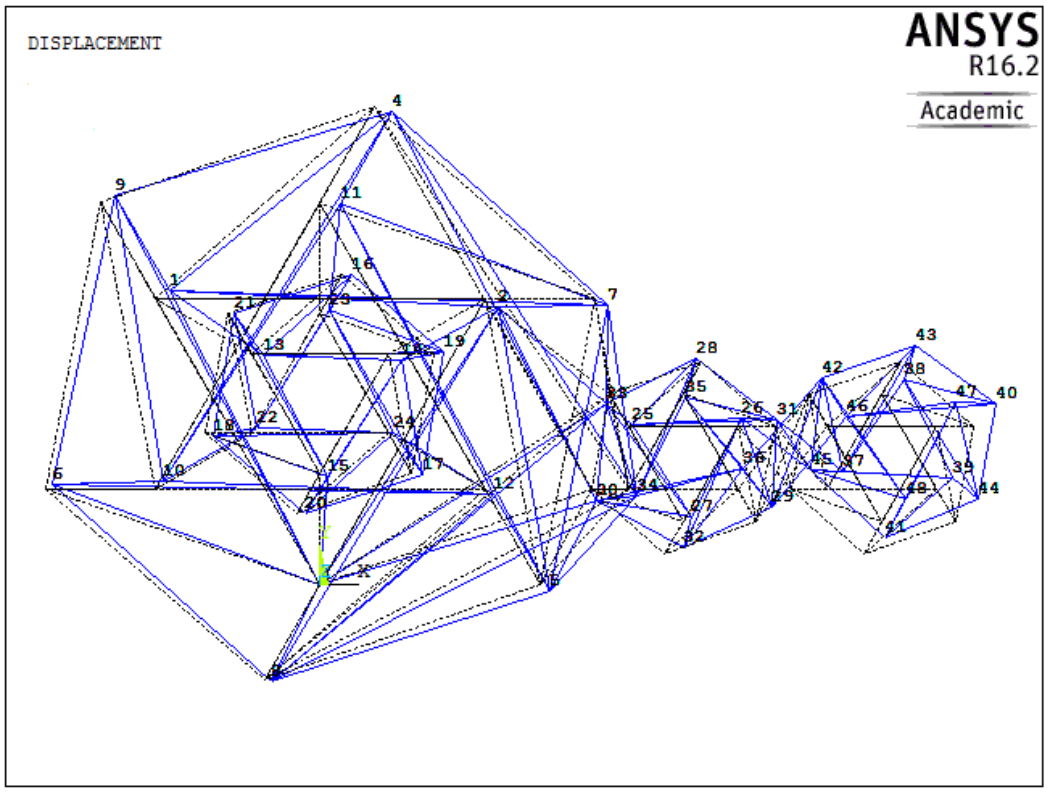

Figure 14 Cell moves sideways (x-y plane)

Below is the flow chart that describes the simulation process for different cases.

Case 1: Cell moves forward for 1 micron

- 1. Apply pre-stress.
- 2. Give forward Nodes 40 and 44 a one micron displacement in the positive x direction, constrain node 40 and node 44 in the y direction.

Case 2: Cell moves forward for 2 micron

- 1. Apply pre-stress.
- 2. Give forward Nodes 40 and 44 a two micron displacement in the positive x direction and constrain node 40 and node 44 in the y direction.

Case 3: Cell encounters the wall

- 1. Apply pre-stress.
- 2. Give forward Nodes 40 and 44 a one micron displacement in the positive x direction and constrain node 40 and node 44 in the y direction.
- 3. Calculate the value of F_3, $F_3 = F_2 – F_1$.
- 4. Apply F_3 to each node and release the constraints for node 40 and node 44 in the y direction.

Case 4: Cell moves up

- 1. Apply pre-stress.
- 2. Give forward Nodes 40 and 44 a one micron displacement in the positive x direction and constrain node 40 and node 44 in the y direction.
- 3. Give node 40 and node 44 a one micron displacement in the positive z direction and release nodes 46, 47 and 48 in the z direction, which were constrained before.
-

Case 5: Cell moves sideways

- 1. Apply pre-stress.
- 2. Give forward Nodes 40 and 44 a one micron displacement in the positive x direction and constrain node 40 and node 44 in the y direction.
- 3. Release the constraints of node 40 and node 44 in the y direction. Then give node 40 and node 44 a one micron displacement in the positive y direction

Figure 15 Flow charts of the simulation processes

3.2 Results

To investigate the relationship between cells' movements and total energy, the strain elastic energy of each element of the model is calculated and added up for each case described above. The total resultant energy for the deformed shape after cells' movements is obtained and summarized in Table 3.

Table 3 Resultant energy values for the final configurations in different cases

Case	Resultant energy (J/m^2)
Cell model with pre-stress only	$0.133*10^{-13}$
Cell moves forward for one micron	$0.212*10^{-12}$
Cell moves forward for two micron	$0.855*10^{-12}$
Cell encounters the wall	$0.382*10^{-12}$
Cell moves up	$0.230*10^{-12}$
Cell moves sideways	$0.291*10^{-12}$

From Table 3, it is easy to see that the least resultant energy is for the case where only pre-stress is introduced. The cell needs to generate internal forces that must lead to an energy increase.

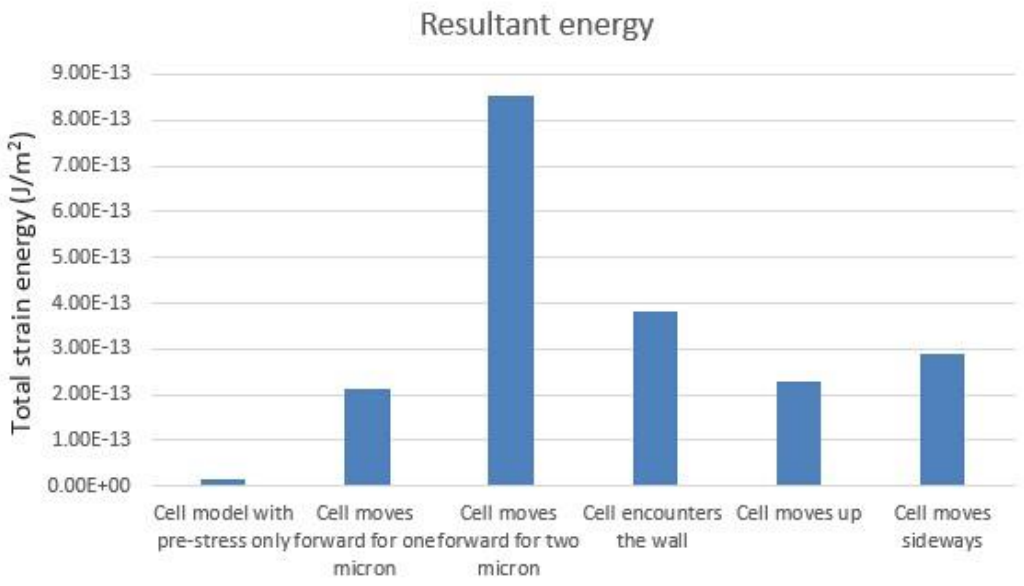

Figure 16 Resultant strain energy for the deformed configuration

Figure 16 illustrates the comparison of the magnitude of the resultant energy value for cells in several cases. The energy of the two micron forward movement is much larger than in the other cases. By comparing the internal elastic energy of a cell moving forward for one micron with two micron, it can be seen that two micron movement needs a significantly larger amount of energy than one micron movement. It indicates that the more distant cells move the larger energy cells need to generate.

In the third case, where the cell encounters the wall, the resultant energy is between the energy needed for one micron and two micron. There must be an energy consuming process when the cell encounters the wall. Some energy is released by this process and it may also lead to a change in shape of the cell. Thus,

it is clear that the resultant energy after encountering the wall is smaller than the resultant energy for two micron forward movement.

In addition, due to the relatively high level of internal elastic energy of a cell encountering the wall compared to the energy of a cell moving up, cells may not stay at the concave corner after encountering the wall, which means the cell has a tendency to leave the concave corner and then moves up to stay on the side wall. An experiment was conducted by Park, *et. al.* in 2009.[10] In this experiment, L929 mouse fibroblast cells were cultured on a surface with a concave microstructure. The experimental results showed that the cells sensed the three-dimensional microscale curvature and actively escaped from the concave corner.

For the cases of upward movement and sideways movement, the resultant energies of both are more than the energy for one micron movement but less than the energy for two micron movements. But compared to the energy for one micron forward movement, the energy increments of these two cases are much less than the increment of two micron movements. This means that the configuration when the cell moves up or sideways is more stable than when the cell directly moves forward for two microns. Thus, the cell has a tendency to move up or sideways. If a large number of cells are observed in the pit substrate, they are expected to move towards the side walls. If a time-lapsed observation is carried out, the cell's density on the side walls might be higher than on the other locations in this pit substrate. A corresponding experiment was conducted by conducted by Kim *et. al.* in 2014.[37] Cells were cultured on micropatterned substrates with pits. After a period of time, the density of the cells was measured

and the result showed that at the side walls it was higher than on the bottom surface. Thus, we can conclude that the results produced by our model match the results generated by other experiments.

To evaluate the effect of movement in the y direction and verify the correctness of this model furthermore, we release constraints for node 40 and 44 in the y direction in each step. A list of new results is observed after running the simulation by following the simulation process described above.

Table 4 Resultant energy values for the final configuration in different case after releasing y-direction constrain

Case	**Resultant energy (J/m^2)**
Cell with pre-stress only	$0.133*10^{-13}$
Cell moves forward for one micron	$0.895*10^{-13}$
Cell moves forward for two micron	$0.325*10^{-12}$
Cell encounters the wall	$0.225*10^{-12}$
Cell moves up	$0.197*10^{-12}$
Cell moves sideways	$0.291*10^{-12}$

After allowing for the edge of the lamellipodium to move in the y direction, the data for the resultant energy in each case will change, except in the first and the last case. The reason is that there is no movement in the y direction in the first case, and in the last case, the value of the movement in the y direction is one micron, which will give out the same value of resultant energy.

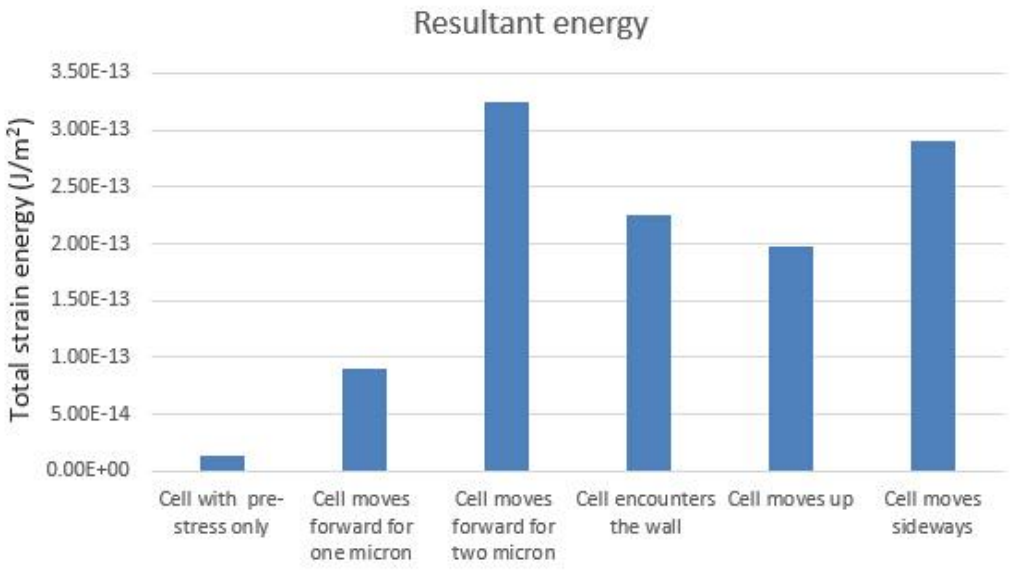

Figure 17 Resultant energy values for the different cases after releasing y-direction constrain

Although the specific values of the resultant energies change, in comparison with the results generated by the cases where the y-direction movement is constrained, the qualitative energy relationship does not change. The resultant energy of two micron forward movements still shows the highest value. The resultant energy of the later three situations is still between one and two micron forward movements. Furthermore, by comparing the energy of the cells encountering the wall with the cells moving upwards, we can conclude that they still have a tendency to leave the concave corner after encountering the wall.

4. A computational model to simulate cell's viscoelasticity

4.1 Cell's viscoelasticity

Living cells' response to the external mechanical stresses as well as cellular deformation are crucial functions.[38] Recent research found that cells exhibit viscoelastic behavior under compression.

The research carried out focused on the stiffness and viscoelastic behavior of adult human mesenchymal stem cells (hMSCs). A BioMEMS device is used to extract the mechanical property of stress relaxation for the stem cell. The experimental process applies a constant displacement to the cell and then measures the corresponding reaction force on the cell.[39]

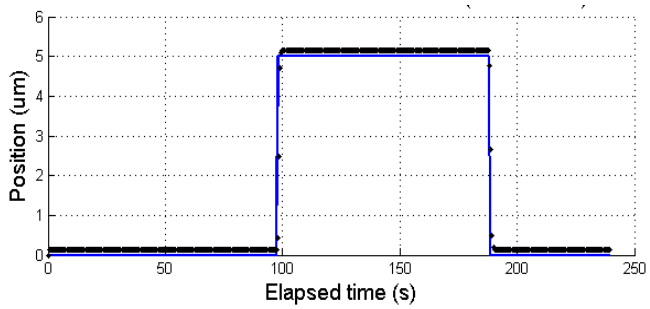

Figure 18 Applied deformation versus time [39]

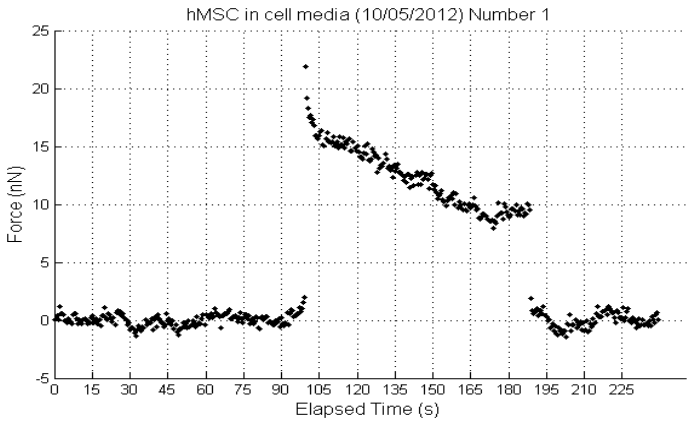

Figure 19 Experimental data for force versus time[39]

In this study, the elastic and viscoelastic properties of hMSC cells were extracted using a standard linear solid model. To fit the force-time curve obtained by the experiment, the standard linear solid model produced a mean value of elastic modulus, E_1 = 0.022 KPa, a modulus of 1.15 KPa for E_2, and a relaxation time which is equal to 29.9 s. The schematic drawing for the Standard Linear Solid Model is shown in Figure 20.

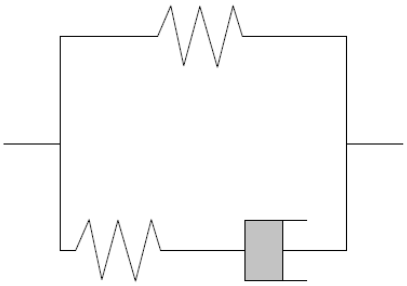

Figure 20 Standard Linear Solid Model

4.2 Simulation Method

A 30-member tensegrity structure was used to simulate cells' viscoelasticity. The viscoelastic properties of the cell need to be defined. The value of the elastic modulus is constant, which is 2.6 GPa for the tensile elements and 1.2 GPa for the compression elements. Then, the parameters that are related to the viscoelastic property are calculated.

In ANSYS APDL, two types of models can be used to simulate viscoelasticity. One is a Maxwell model, another is a Prony series model. Below are the schematic drawings (Figure 21 and 22) for the two models.

Figure 21 Maxwell model

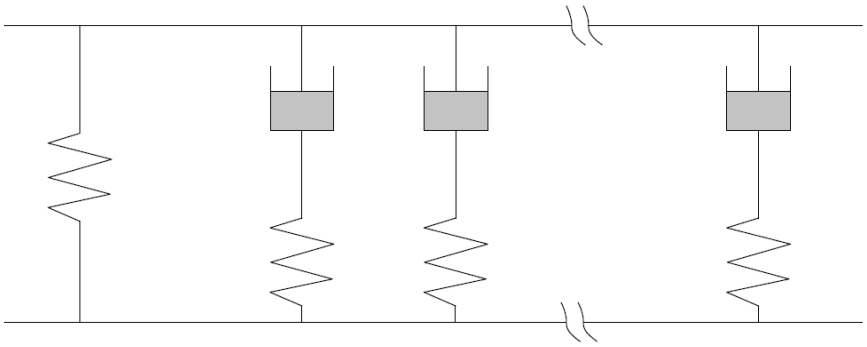

Figure 22 Schematic for Prony series model

The Prony series model is composed of a free spring and an infinite series of springs and dashpots in parallel. By comparing the the Prony series with a standard linear solid model, it is obvious if the Prony series only contains one spring with one dashpot in parallel, the Prony model can also represent a standard linear solid model used in the experimental data curve-fitting.

Therefore, the Prony series approach is selected in this study. The mathematical representation for the Prony series is,[40]

$$E(t) = E_0 + \sum_{n=1}^{\infty} E_n \exp(-\frac{t}{\tau}) \qquad (10)$$

Using the one-term Prony series model to simulate the standard linear solid model, the mathematic representative formula changes to:

$$E(t) = E_1 + E_2 \exp(-\frac{t}{\tau}) \quad (11)$$

From the data produced by the standard linear solid model, we have E_1 = 0.022, E_2 = 1.15 kPa and τ = 29.9 s, thus,

$$E(t) = 0.022 + 1.15 * \exp(-\frac{t}{29.9}) \quad (12)$$

To use these parameters into ANSYS APDL, we define,

$E_0 = E_1 + E_2 = 0.022 + 1.15 = 1.172$ (13)

The input parameters are calculated as,

$$\alpha_1^G = \alpha_1^K = \frac{E_2}{E_0} = 0.98 \quad (14)$$

$$\tau = 29.9 \quad (15)$$

Below is the ANSYS APDL command code representation,

```
TB, PRONY, 1, 1, SHEAR

TBDATA, 1, 0.98, 29.9

TB, PRONY, 1, 1, BULK

TBDATA, 1, 0.98, 29.9
```

Figure 23 ANSYS APDL command code to define the cell viscoelastic properties

After the material properties are defined, we change the analysis type from static analysis to transient analysis and then proceed according to the following steps.

- 1. Apply pre-stress
- 2. Give the nodes on the top-surface, which are node 10, 11 and 12, a 5 micron displacement in the negative z direction
- 3. Keep the displacement.
- 4. Obtain the reaction force versus time for the cell.

All simulations are running on the computer with an i7-4600U CPU and 8GB of RAM.

4.3 Results

Since the experimental elapsed time is around 100 seconds, we implement our simulation that elapsed time is 100 seconds. The obtained results (Figures 24) show the plots of reaction force versus time.

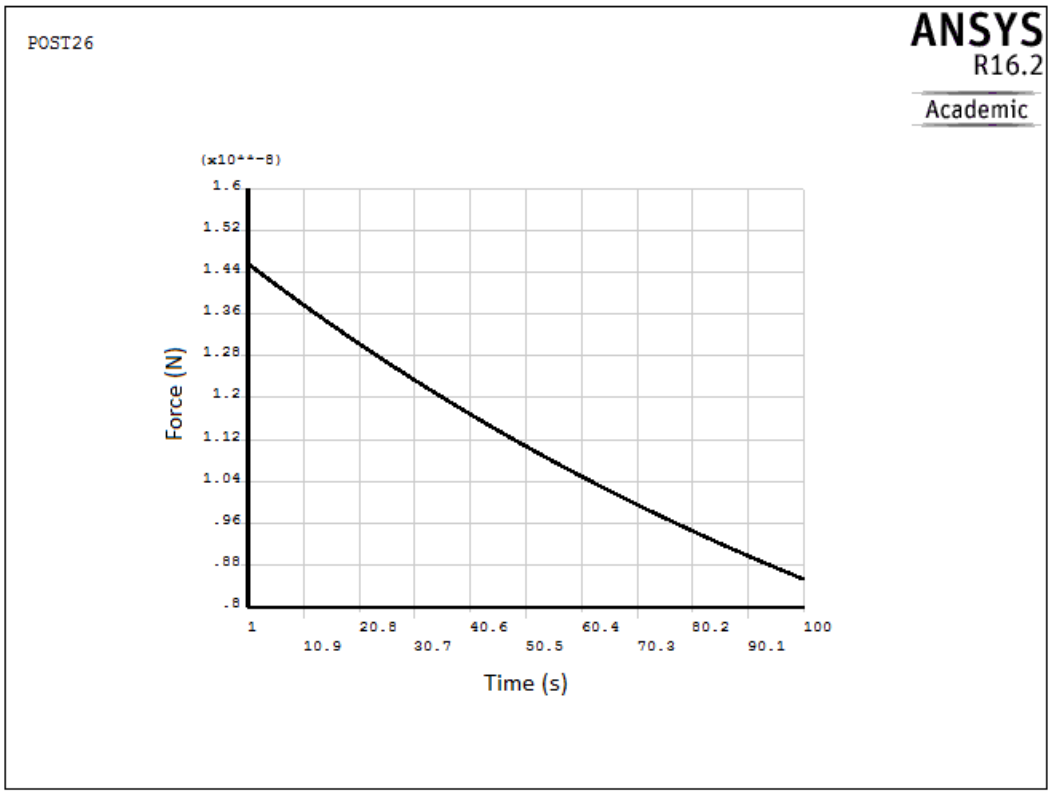

Figure 24 Reaction force versus time (elapsed time = 100s)

We obtain the force values at both the start and end times from the experimental data (Figure 19), as well as the simulation plot that elapsed time is 100 seconds (Figures 24), then compare these values by calculating the ratio of initial force value to final force value (Table 5).

Table 5 The comparison of the experimental results and the simulation results

	Initial force value	Final force value	Ratio of initial force value to final force value
Case 1:experimental results	18 nN	9 nN	2.00
Case 2: Simulation results (Elapsed time: 1 to 100 seconds)	14.5 nN	8.4 nN	1.72

In the experimental results, the initial force is 18 nN, the final force is 9 nN, the ratio of initial force to final force is 2.00. From the simulation results, the initial force is 14.5 nN and the final force is 8.4 nN. The ratio of initial force to final force is 1.72. Although the specific force values have some discrepancies between the experimental results and the simulation results, the ratio value obtained by our model approach the experimental result. This indicates this tensegrity viscoelastic model can illustrate a very similar stress-relaxation curve compared to the curve which is directly generated by the experiment.

To evaluate the effect of pre-stress on this viscoelastic cell model, it is changed from $0.80*10^{-14}$ N for tensile force and $-1.92*10^{-14}$ N for compressional force, to $1.60*10^{-14}$ N for tensile force and $-3.92*10^{-14}$ N for compressional force. The resultant plot is shown in Figure 25.

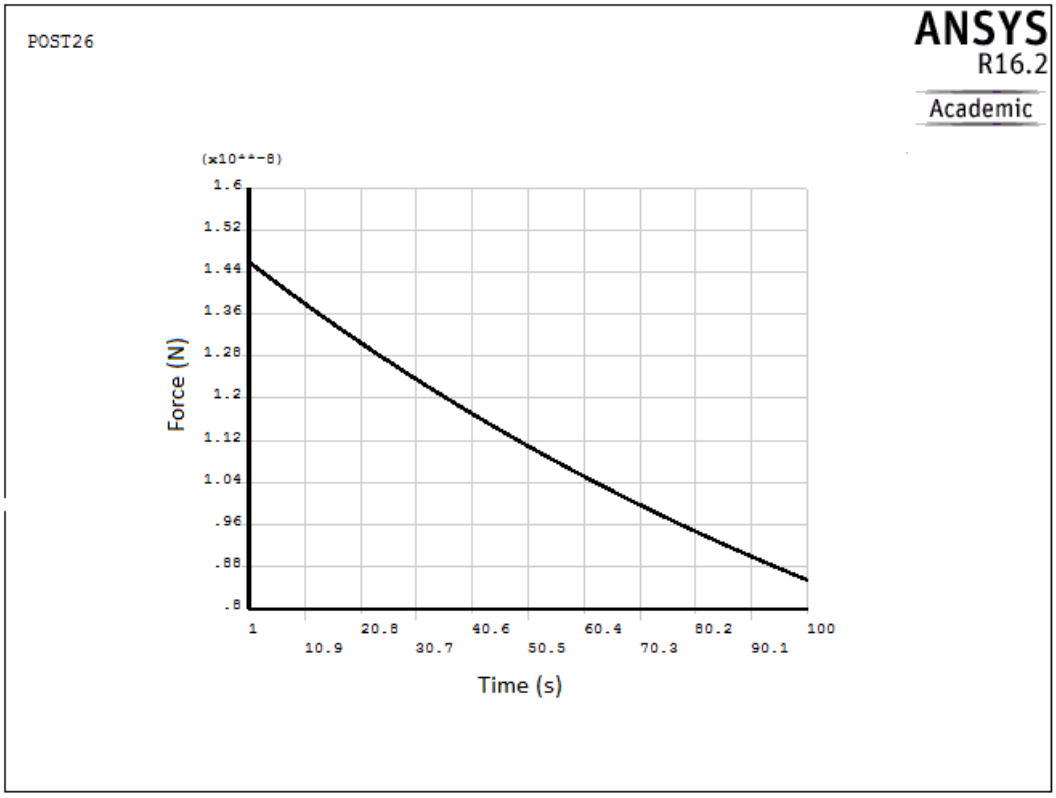

Figure 25 Reaction force versus time after pre-stress change (elapsed time = 100s)

By comparing Figure 24 with Figure 25, no distinct changes between them are observed, which means the pre-stress value has an insignificant effect on this viscoelastic cell model.

Although the pre-stress values do not impact the results significantly, the parameters of the Prony series that define the elements' material properties influence the results significantly. A 2-term Prony series model uses $\alpha_1 = 0.074$, $\alpha_2 = 0.306$, $\tau_1 = 2.24$ and $\tau_2 = 3.75$. The resultant plot shows a curve with a more evident curvature which illustrates an obvious viscoelastic behavior (Figure 26).

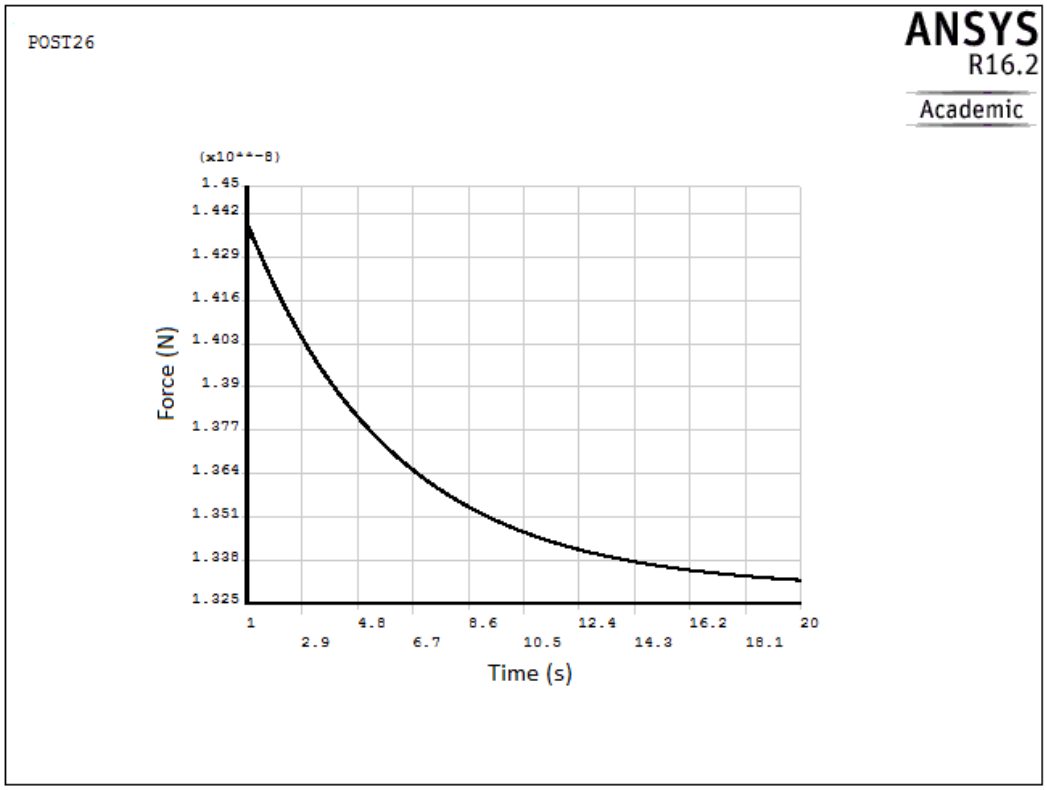

Figure 26 Reaction force versus time for 2-term Prony series model (elapsed time = 20s)

If we show the plot from 0.1 second to 20 second, we find some oscillations closed to the starting time. In fact, since we use a transient analysis, which is a nonlinear analysis in ANSYS APDL, every plot we obtained might have some oscillations initially. However, the oscillations vanish before time = 1 second.

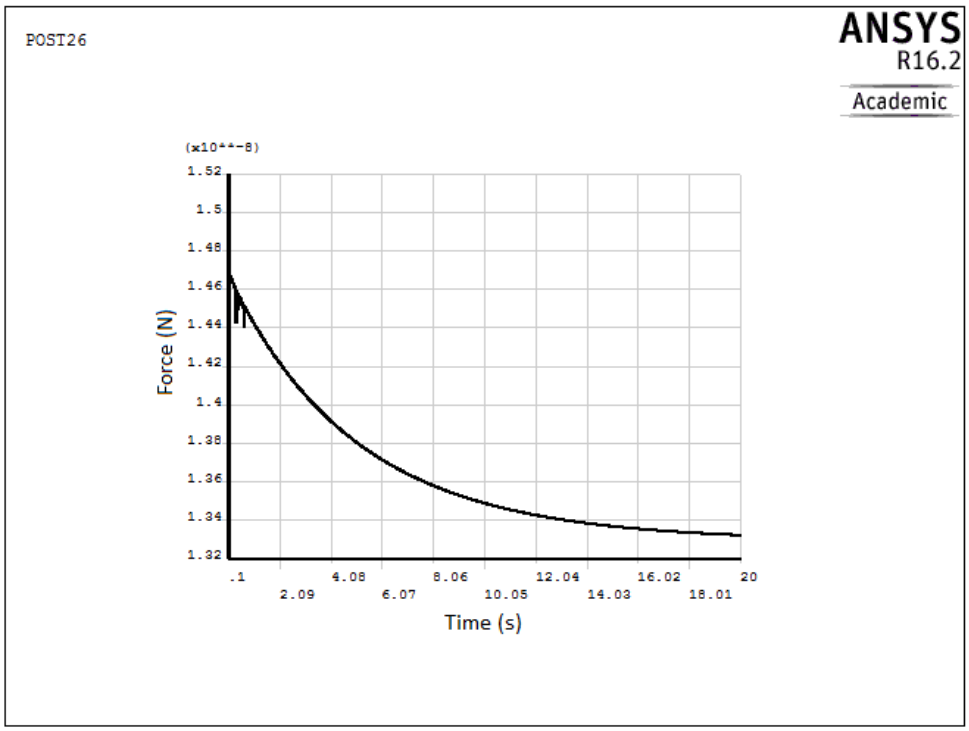

Figure 27 Reaction force versus time for 2-term Prony series model starting from 0.1 second (elapsed time = 20s)

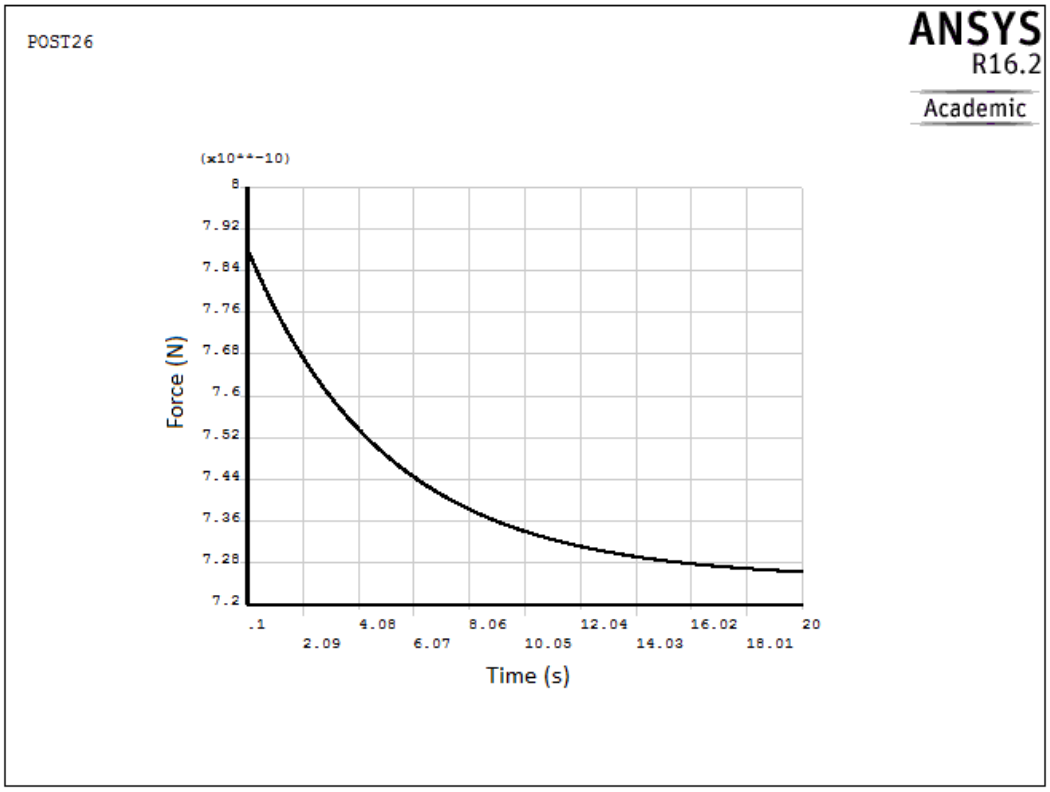

Figure 28 reaction force versus time for 2-term Prony series model (apply one micron displacement)

There are some oscillations from time = 0.1 second to time = 1 second (Figure 27). The oscillations occur due to the transient analysis. Applying a five micron displacement leads to the velocity and acceleration change. In transient analysis, initial velocity and acceleration have to be taken into account. Moreover, five micron is a relatively large deformation compared to the total height of our model. If we apply only one micron to this model, the resulting behavior curve is smooth, without oscillations (Figure 28). These two reasons result in the fact that the iteration cannot converge immediately after displacement is applied. But usually, after a few seconds, the curve will be smooth without oscillations.

A three-term Prony series model is also introduced. The parameters are defined as, E_{total} = 1.153 MPa, E_0 = 0.250 MPa, E_1 = 0.208 MPa, E_2 = 0.272 MPa, E_3 = 0.423 MPa, λ_1 = 1.600 (1/s), λ_2 = 0.118 (1/s), λ_3 = 0.011 (1/s) (Patrick A. Smyth, 2013).[41]

The ANSYS APDL inputting parameters are: α_1 = 0.18, α_2 = 0.24, α_3 = 0.37, τ_1 = 0.675, τ_2 = 8.475, τ_3 = 90.91. After applying a 5 micron constant negative displacement, the corresponding plot is shown in Figure 29.

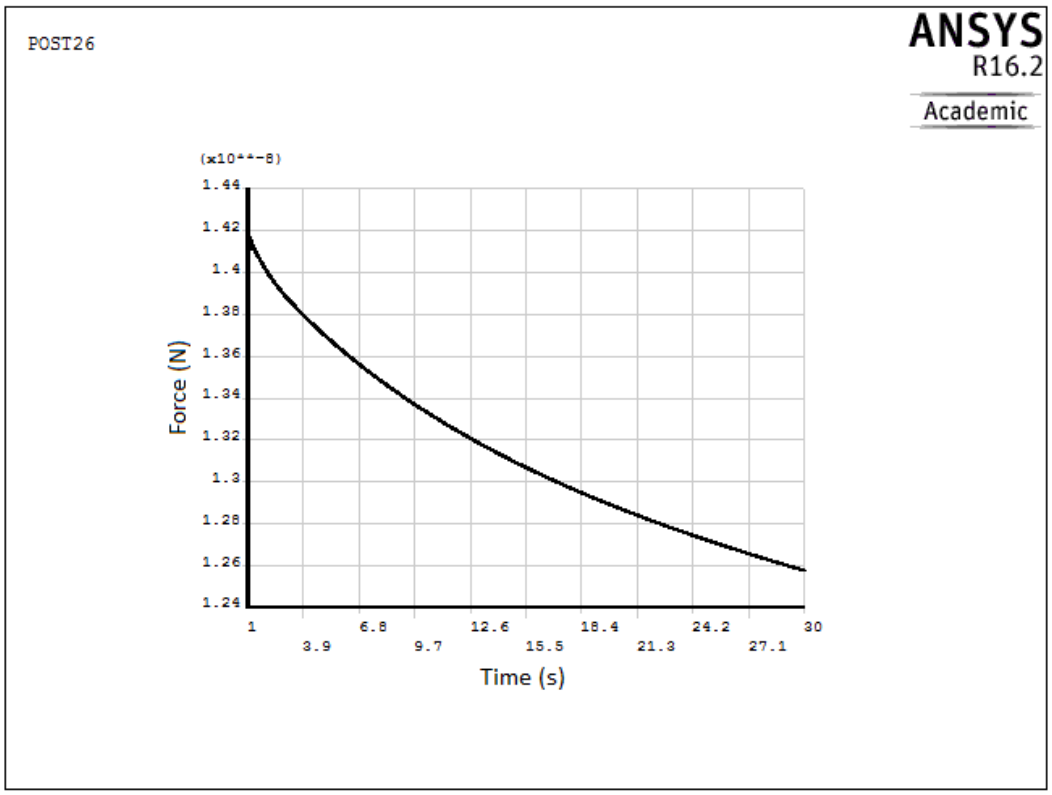

Figure 29 Reaction force versus time for 3-term Prony series model (elapsed time = 30s)

By comparing the plot generated by the one-term Prony series model with this two-term model, the results for the two-term model shows a more evident curvature and then approach to a relatively horizontal direction. It can be

concluded that the force decreases over a short period of time and remains almost constant later on, which shows a typical stress relaxation behavior.

5. Discussion

This study is divided into two parts, the first part focuses on cells' movement, and the second part focuses on cells' viscoelasticity.

For the study of cells' movement, to simulate the movement on a substrate, a new type of tensegrity model is developed. This new model not only contains the cells' cytoskeleton but also contains the nucleus and the lamellipodium. Every time the cell wants to move, the lamellipodium is first extended then it pulls the main cell body forward. By modeling the cell located in the middle of a pit, several cases are investigated: cell movement forward along the surface for one micron and two microns, cell movement forward and movement up when on a vertical wall, cell movement forward and then movement sideways when encountering the wall, and cell movement forward and then encountering the wall.

From the minimizing the elastic internal energy point of view, the cell has a higher probability of moving to and staying in a lower energetic state. The resultant energy is calculated when the cell moves to different locations. In this study, one micron forward movement leads to minimum energy while two micron forward movement leads to maximum energy compared with all other cases. The resultant energy of the upward and sideways movement is less than the energy of two micron movement. Since both the upward and the sideways movements result in the situation that cells locate on the side walls, it can be concluded that cells have a tendency to move to and locate on side walls when they are in a pit.

The situation when cells encounter the wall is also observed. If cells encounter the wall during their moving path they have potential of the remaining

forces that were not utilized during planned motion. To simulate the wall encountering, the remaining forces are calculated and applied when cells encounter the wall after a certain distance movement. By comparing the resultant energy of the cell encountering the wall with all other cases, the case for the cell's upward movement leads to lower energy than when encountering the wall, which indicates cells may ultimately leave the concave corner and then move up and locate on the side walls.

The related experimental results were presented by Kim *et. al.*[37] in the study of the influence of surface topography on the human epithelial cell response to micropatterned substrates with convex and concave architectures. In this study, a micropatterned substrate with pit architecture was established to assess the responses of human epithelial cells and investigate the cells' distribution. A number of cells were cultured on micropatterned substrates with pit. After a period of time, the density of the cell was measured and the result showed that the density of the cell on the side walls was higher than at the bottom. In addition, it was observed that the formation of the stress fiber with the lamellipodium and filopodium were seldom seen at the concave corner of the pit substrate, which indicated the cells hardly stayed in the corner and had a tendency to leave the concave corner. The experimental observation clearly indicates that our model and expectations make sense.

For the cells' viscoelasticity study, a 30-member tensegrity model is used. The Prony series model defines 24 cable members as viscoelastic materials. We derive the one-term Prony series ANSYS APDL input parameters based on the

experimental results presented by Moghimi *et. al.*[39] in the study of biomechanical characterization of single suspended human mesenchymal stem cells under compression. Next, we apply five micron constant negative displacement to the cell. The plot of reaction force versus time is obtained after simulation ends. By comparing our simulation results with the experimental results, the plot obtained by this computational model fits the curve obtained by the experiment.

To evaluate the relationship between the Prony series parameters and viscoelastic property two-term Prony series and three-term Prony series model are introduced. The result shows different values of parameters and different numbers of terms do have an influence on the stress decreasing speed and also have an effect on the curvature of the relaxation plot.

In conclusion, the new model with a nucleus and a lamellipodium created in this study provides a reasonable explanation for the tendency of cells' movement when a cell is in a pit. Moreover, the tensegrity structure can also be used to simulate cells' viscoelastic behavior by employing transient analysis and using proper Prony series parameters.

6. Conclusion

This study can be divided into two parts: the study of cell's movement and the study of cell's viscoelastic property.

In the first part, a computational cell model with a nucleus and a lamellipodium is proposed based on tensegrity structure. The cell is initially placed on a flat surface and then we model its movement within the pit substrate. According to our model, the cell's upward and sideways movement would lead to a lower strain energy than if a cell directly moves along a straight line, such as in a two micron forward movement. In addition, in comparison with the cell's upward movement, in the case that the cell encounters the wall leads to higher energy. Thus, a conclusion is generated that the cell has a tendency to move and stay on the side walls in a pit. In addition, cells also have a tendency to leave the concave corner and then settle down on the side. Therefore, this newly created cell model is a valuable tool for investigating cells' responses to surface topography.

In the second section, a 30-member tensegrity model is used. The viscoelastic properties of the filament members is defined by the Prony series. Based on the experimental data, the parameters of the Prony series are calculated and used in the study. The results show a very similar trend and data relationship compared with the experimental data. Further investigation finds that the pre-stress of tensegrity has little influence on viscoelastic properties. In addition, by using the two-term or three-term Prony series, the plot curve shows a more evident curvature and then approach to a relatively horizontal direction, which

shows a typical stress relaxation behavior. In conclusion, this study shows the feasibility of the tensegrity model to simulate cells' viscoelastic behavior.

Reference

[1] Stamenović, Dimitrije, and Donald E. Ingber. "Tensegrity-guided self-assembly: from molecules to living cells." Soft Matter 5.6 (2009): 1137-1145.

[2] Gure, Ali O., Türeci, Ö., Sahin, U., Tsang, S., Scanlan, M.J., Jäger, E., Knuth, A., Pfreundschuh, M., Old, L.J. and Chen, "SSX: a multigene family with several members transcribed in normal testis and human cancer." International journal of cancer 72.6 (1997): 965-971.

[3] Chen, Christopher S., Christopher S., Milan Mrksich, Sui Huang, George M. Whitesides, and Donald E. Ingber.. "Geometric control of cell life and death." Science 276.5317 (1997): 1425-1428.

[4] Ingber, Donald E. "Cellular basis of mechanotransduction." Biological Bulletin 194.3 (1998): 323-327.

[5] Pelham, Robert J., and Yu-li Wang. "Cell locomotion and focal adhesions are regulated by substrate flexibility." Proceedings of the National Academy of Sciences 94.25 (1997): 13661-13665.

[6] Vogel, Viola, and Michael Sheetz. "Local force and geometry sensing regulate cell functions." Nature reviews molecular cell biology 7.4 (2006): 265-275.

[7] Schroeder, Julian I., Gethyn J. Allen, Veronique Hugouvieux, June M. Kwak, and David Waner. "Guard cell signal transduction." Annual review of plant biology 52.1 (2001): 627-658.

[8] Li, S., Guan, J. L, and Chien, S. (2005). Biochemistry and biomechanics of cellmotility. Annu. Rev. Biomed. Eng., 7, 105-150.

[9] Sheetz, M. P., Felsenfeld, D. P., and Galbraith, C. G. (1998). Cell migration: regulation of force on extracellular-matrix-integrin complexes. Trends in cell biology, 8(2), 51-54.

[10] Park, Joong Yull, Dae Ho Lee, Eun Joong Lee, and Sang-Hoon Lee. "Study of cellular behaviors on concave and convex microstructures fabricated from elastic PDMS membranes." Lab on a Chip9.14 (2009): 2043-2049.

[11] Lim, C. T., E. H. Zhou, and S. T. Quek. "Mechanical models for living cells—a review." Journal of biomechanics 39.2 (2006): 195-216.

[12] Coughlin, M. F., and Stamenović, D. (2003). A prestressed cable network model of the adherent cell cytoskeleton. Biophysical journal, 84(2), 1328-1336.

[13] Karcher, H., Lammerding, J., Huang, H., Lee, R. T., Kamm, R. D., and Kaazempur-Mofrad, M. R. (2003). A three-dimensional viscoelastic model for

cell deformation with experimental verification. Biophysical journal, 85(5), 3336-3349.

[14] Shieh, A. C., and Athanasiou, K. A. (2003). Principles of cell mechanics for cartilage tissue engineering. Annals of biomedical engineering, 31(1), 1-11.

[15] Gan, Y. X., Chen, C., and Shen, Y. P. (2005). Three-dimensional modeling of the mechanical property of linearly elastic open cell foams. International Journal of Solids and Structures, 42(26), 6628-6642.

[16] Gong, L., and Kyriakides, S. (2005). Compressive response of open cell foams Part II: Initiation and evolution of crushing. International Journal of Solids and Structures, 42(5), 1381-1399.

[17] Gong, L., Kyriakides, S., and Jang, W. Y. (2005). Compressive response of opencell foams. Part I: Morphology and elastic properties. International Journal of Solids and Structures, 42(5), 1355-1379.

[18]Cohen, Albert, Ronald A. DeVore, and Reinhard Hochmuth. "Restricted nonlinear approximation." Constructive Approximation 16.1 (2000): 85-113.

[19]Hochmuth, R.M., 2000. Micropipette aspiration of living cells. Journal of biomechanics, 33(1), pp.15-22.

[20] Evans, E., and A. Yeung. "Apparent viscosity and cortical tension of blood granulocytes determined by micropipet aspiration." Biophysical journal 56.1 (1989): 151.

[21] Yeung, A., and E. Evans. "Cortical shell-liquid core model for passive flow of liquid-like spherical cells into micropipets." Biophysical Journal 56.1 (1989): 139-149.

[22] Linnan, M.J., Mascola, L., Lou, X.D., Goulet, V., May, S., Salminen, C., Hird, D.W., Yonekura, M.L., Hayes, P., Weaver, R. and Audurier, A., "Epidemic listeriosis associated with Mexican-style cheese." New England Journal of Medicine 319.13 (1988): 823-828.

[23] Winter, H. Henning, and Francois Chambon. "Analysis of linear viscoelasticity of a crosslinking polymer at the gel point." *Journal of Rheology (1978-present)* 30.2 (1986): 367-382.

[24] Coughlin, M. F., and Stamenovic, D. (1998). A tensegrity model of the cytoskeleton in spread and round cells. Journal of biomechanical engineering, 120(6), 770-777.

[25] Wendling, S., Oddou, C., and Isabey, D. (1999). Stiffening response of a cellular tensegrity model. Journal of theoretical biology, 196(3), 309-325.

[26] Canadas, Patrick, Valerie M. Laurent, Christian Oddou, Daniel Isabey, and Sylvie Wendling. "A cellular tensegrity model to analyse the structural viscoelasticity of the cytoskeleton." Journal of Theoretical Biology 218.2 (2002): 155-173.

[27] Fuller, Buckminster. "Tensegrity." Portfolio Artnews Annual 4 (1961): 112-127.

[28] Lim, C. T., E. H. Zhou, and S. T. Quek. "Mechanical models for living cells—a review." Journal of biomechanics 39.2 (2006): 195-216.

[29] Wee, Hwabok, and Arkady Voloshin. "Modal analysis of a spreading osteoblast cell in culturing." Bioengineering Conference (NEBEC), 2012 38th Annual Northeast. IEEE, 2012.

[30] Shen, B., Qin, D.Q., Wang, X., Zhang, Y., Shekastehband, B., Li, X.Y., Li, H.W., Li, G., Hulbert, G.M., Wu, C. and Luo, Y., "Dynamic Analysis of Spatial Structures." (2008).

[31] Michal Maciej Bartosik, 2011, photograph, viewed on 17 April 2016, < https://tensegrity.wikispaces.com/Tensegrity+Lights+by+Bartosik >

[32] Yalcintas, E.P., Hu, J., Liu, Y. and Voloshin, A. "Modeling cell spreading and alignment on micro-wavy surfaces." CMES: Computer Modeling in Engineering and Sciences 98.2 (2014): 151-180.

[33] Ingber, Donald E., Ning Wang, and Dimitrije Stamenović. "Tensegrity, cellular biophysics, and the mechanics of living systems." Reports on Progress in Physics 77.4 (2014): 046603.

[34] Jie sheng, "A computational model of cell movement linked to Substrate Rigidity", Master thesis, Lehigh University, 2016

[35] Voloshin, Arkady. "Modeling cell movement on a substrate with variable rigidity." International Journal of Biomedical Engineering and Science (IJBES), Vol. 3, No. 1, January (2016): 19-36.

[36] Gittes, F., Mickey, B., Nettleton, J. and Howard, J. (1993) "Flexural rigidity of microtubules and actin filaments measured from thermal fluctuations in shape", The Journal of cell biology, 120(4), 923-934.

[37] Kim, Mee-Hae, Yoshiko Sawada, Masahito Taya, and Masahiro Kino-oka. "Influence of surface topography on the human epithelial cell response to micropatterned substrates with convex and concave architectures." Journal of biological engineering 8.1 (2014): 1.

[38] Chumakov, I., Blumenfeld, M., Guerassimenko, O., Cavarec, L., Palicio, M., Abderrahim, H., Bougueleret, L., Barry, C., Tanaka, H., La Rosa, P. and Puech,

A., 2002. Genetic and physiological data implicating the new human gene G72 and the gene for D-amino acid oxidase in schizophrenia.Proceedings of the National Academy of Sciences, 99(21), pp.13675-13680.

[39] Moghimi, Jedlicka, Tatic-Lucic, "Biomechanical characterization of single suspended human mesenchymal stem cells under compression." 2016, unpublished manuscript, Lehigh University, Bethlehem, PA.

[40] Park, S.W. and Schapery, R.A., 1999. Methods of interconversion between linear viscoelastic material functions. Part I—A numerical method based on Prony series. International Journal of Solids and Structures, 36(11), pp.1653-1675.

[41] Patrick A. Smyth, "Viscoelastic behavior of articular cartilage in unconfined compression", Master thesis, Georgia institute of Technology, 2013.

Vita

Kaiyuan Peng was born in Hefei, China on February 4, 1992 as the son of Daisheng Peng and Xiaoling Yang. He received a Bachelor of Engineering degree in Mechanical Engineering from Beijing University of Chemical Technology, in June, 2014, then joined the Master of Science graduate program of the Department of Mechanical Engineering and Mechanics at Lehigh University in Bethlehem, Pennsylvania. He was advised for this Master's thesis by Dr. Arkady Voloshin.